Cell Reports
Methods

Article

Long-term, high-resolution *in vivo* calcium imaging in pigeons

Graphical abstract

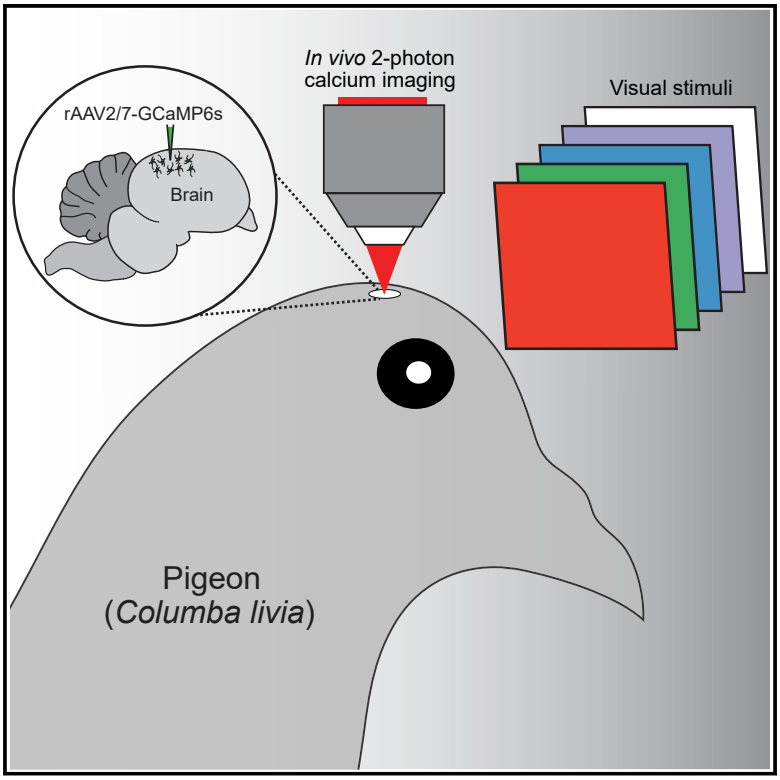

Authors

Simon Nimpf, Harris S. Kaplan, Gregory C. Nordmann, Thomas Cushion, David A. Keays

Correspondence

nimpf@biologie.uni-muenchen.de (S.N.), keays@biologie.uni-muenchen.de (D.A.K.)

In brief

Nimpf et al. report the development of *in vivo* 2-photon calcium imaging in awake pigeons. Imaging of neuronal populations in the pigeon forebrain is achieved using the genetic calcium indicator GCaMP6s delivered by the recombinant adeno-associated virus rAVV2/7. This technique provides opportunities to investigate avian sensory and cognitive biology.

Highlights

- Establishment of *in vivo* 2-photon calcium imaging in awake pigeons
- rAAV2/7 drives efficient expression of GCaMP6s in the pigeon forebrain
- Neurons in the visual Wulst are responsive to color stimuli

Nimpf et al., 2024, Cell Reports Methods *4*, 100711
February 26, 2024
https://doi.org/10.1016/j.crmeth.2024.100711

CellPress

Cell Reports Methods

CellPress
OPEN ACCESS

Article

Long-term, high-resolution *in vivo* calcium imaging in pigeons

Simon Nimpf,[1,*] Harris S. Kaplan,[2] Gregory C. Nordmann,[1] Thomas Cushion,[3] and David A. Keays[1,3,4,5,*]
[1]Division of Neurobiology, Faculty of Biology, Ludwig-Maximilian-University Munich, Planegg-Martinsried, 82152 Munich, Germany
[2]Harvard University, Department of Molecular and Cellular Biology, 16 Divinity Avenue, Cambridge, MA 02138, USA
[3]University of Cambridge, Department of Physiology, Development & Neuroscience, Downing Street, Cambridge CB2 3EG, UK
[4]Research Institute of Molecular Pathology, Vienna Biocenter, Campus-Vienna-Biocenter 1, Vienna 1030, Austria
[5]Lead contact
*Correspondence: nimpf@biologie.uni-muenchen.de (S.N.), keays@biologie.uni-muenchen.de (D.A.K.)
https://doi.org/10.1016/j.crmeth.2024.100711

MOTIVATION *In vivo* 2-photon calcium imaging has emerged as a key technology in neuroscience providing fundamental insight into how information is encoded within defined neuronal circuits. A product of advancements in both optics and genetically encoded calcium indicators, it is now possible to interrogate large neural networks with single-cell resolution over long timescales in awake, behaving animals. While widely used in mammals, this method is underutilized in birds. To address this, we set out to establish calcium imaging in pigeons.

SUMMARY

In vivo 2-photon calcium imaging has led to fundamental advances in our understanding of sensory circuits in mammalian species. In contrast, few studies have exploited this methodology in birds, with investigators primarily relying on histological and electrophysiological techniques. Here, we report the development of *in vivo* 2-photon calcium imaging in awake pigeons. We show that the genetically encoded calcium indicator GCaMP6s, delivered by the adeno-associated virus rAAV2/7, allows high-quality, stable, and long-term imaging of neuronal populations at single-cell and single-dendrite resolution in the pigeon forebrain. We demonstrate the utility of our setup by investigating the processing of colors in the visual Wulst, the avian homolog of the visual cortex. We report that neurons in the Wulst are color selective and display diverse response profiles to light of different wavelengths. This technology provides a powerful tool to decipher the operating principles that underlie sensory encoding in birds.

INTRODUCTION

Over the last century, *Aves* have served as a valuable model species in the fields of sensory, cognitive, and behavioral science.[1–4] Pigeons, for example, are able perform cognitively challenging tasks such as categorization of visual objects, are able to generalize learned information when confronted with new datasets, exhibit complex courting behaviors, perceive UV light, hear infrasound, and detect magnetic fields.[5–11] It is becoming increasingly clear that, despite having a vastly different brain organization, birds' cognitive abilities are on par with those of higher mammals, making them ideal models for the study of evolutionary and comparative neurophysiology.[12] Nevertheless, we understand little of the neuronal circuits that underpin higher cognitive and sensory functions in avian species.[13] To date, most studies have either relied on electrophysiological techniques, which are limited in the number of neurons that can be recorded and reliably tracked across days, or on functional imaging techniques that lack cellular resolution.[14–19] Previous studies in zebra finches have demonstrated the utility of calcium imaging in songbirds, providing novel functional insight into circuits associated with singing.[20–22] We therefore set out to develop *in vivo* 2-photon calcium in pigeons (*Columba livia*), a species well known for its impressive sensory and cognitive abilities.[23,24]

RESULTS

Infrastructure for *in vivo* 2-photon calcium imaging in pigeons

To perform *in vivo* calcium imaging experiments in pigeons, we first set up the necessary microscopy infrastructure. The custom 2-photon laser scanning microscope platform consists of a femtosecond-pulsed, long-wavelength tunable laser (680–1,080 nm), a 8 kHz resonant scanning mirror, a galvanometer mirror, an electrically tunable lens, a custom 3D-printed

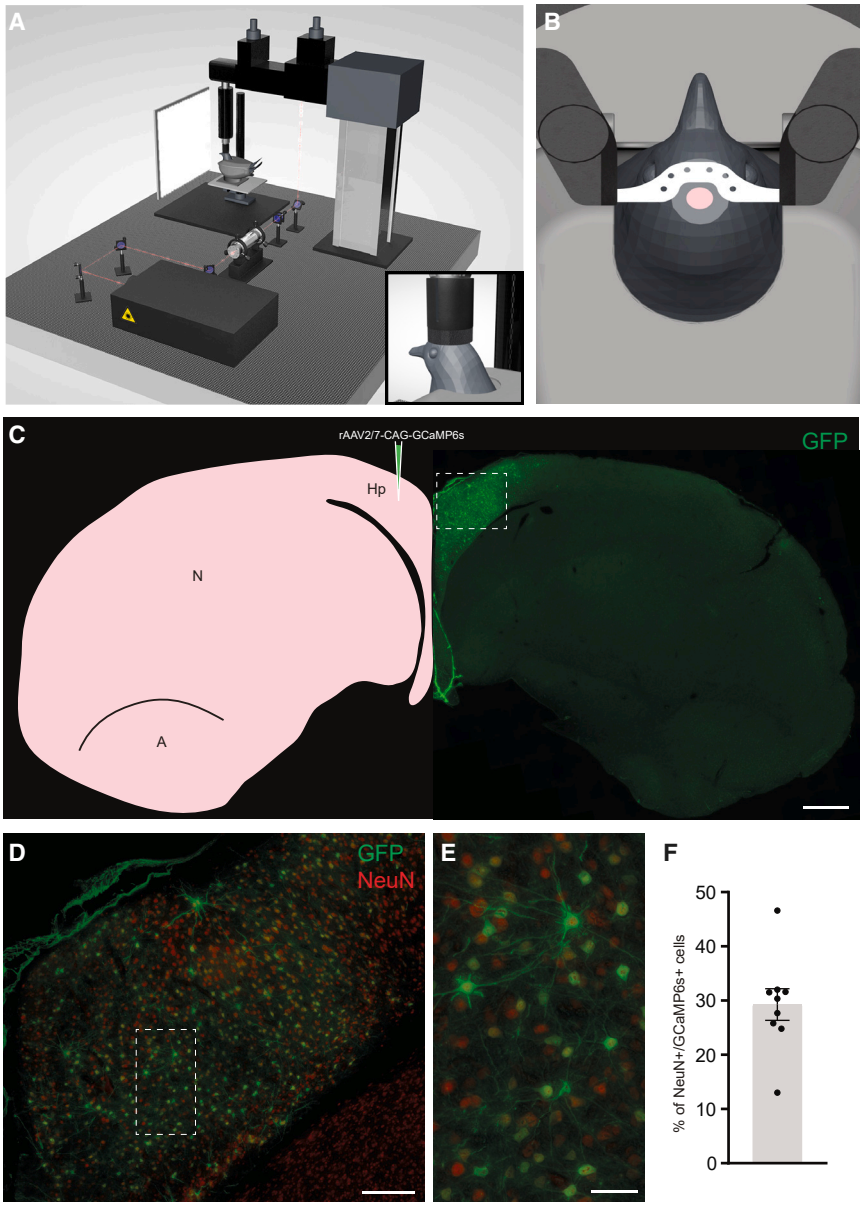

Figure 1. *In vivo* 2-photon calcium imaging setup and viral delivery of GCaMP6s in the pigeon dorsal forebrain

(A) The calcium imaging setup consists of a resonant scanning 2-photon microscope, a femtosecond-pulsed laser, an animal stage, and an LED wall facing the pigeon. The inset shows a custom-made device, which can be attached to the microscope objective to prevent light contamination.

(B) The bird is immobilized under the microscope using a 3D-printed body harness and two head clamps.

(C) Schematic of the pigeon forebrain showing the location of viral injection (left) and a corresponding brain section showing GCaMP6s expression 3 weeks after AAV injection stained with a GFP antibody (right).

(D and E) Double staining using antibodies against GFP (green) and the pan-neuronal marker NeuN (red).

(F) Graph showing the percentage of GFP/NeuN double-positive neurons in a defined region around the injection site of 3 birds (3 sections per bird).

Data are presented as mean ± SEM. Scale bars: 1 mm in (C), 200 μm in (D), and 50 μm in (E). Hp, hippocampus; N, nidopallium; A, arcopallium.

See also Figures S1 and S2.

objective lens extension tube, and a 16× water immersion objective (Figure 1A). Fluorescent light is collected using GaAsP photomultiplier tubes. The system is furthermore equipped with motion control allowing 100 mm travel in x, y, and z and is controlled by Scanbox acquisition software (Neurolabware, Los Angeles, CA, USA) run on a Dual 6-core, 3.4 GHz CPU, 128 GB RAM computer. The motion control system records the x, y, and z coordinates of the microscope, enabling imaging of the same location at a later time point. To prevent external light from entering the microscope path, we designed a device made out of black hard plastic and black foam material at the bottom, which could be attached to the microscope objective (Figure 1A, inset). We constructed a customized animal stage that consists of a 3D-printed body harness and two head clamps to immobilize the pigeon under the microscope (Figure 1B).

Assessing the optimal viral vector for gene delivery in the pigeon forebrain

The recording of neuronal activity using 2-photon microscopy requires the introduction of a calcium indicator into the brain region of interest. As transgenic pigeons are currently unavailable, we elected to use a viral-vector-mediated gene delivery system to introduce a genetically encoded calcium indicator into the brain in an anatomically targeted manner. Pseudotyped recombinant adeno-associated viral vectors (rAAVs) have been extensively used for gene delivery in diverse mammalian species, and the transduction efficacy of various serotypes for different brain regions and cell types has been well described.[25–28] Implementing common viral gene delivery strategies in birds has proven difficult, and little is known about the tropism and effectiveness of different AAV serotypes in the pigeon brain.[29–31] We therefore set out to identify the optimal viral vector for gene delivery in the pigeon forebrain, focusing on the dorsal pallium. Recombinant pseudotyped vectors (rAAV1–9), driving the expression of the reporter gene GFP under the control of the CMV promoter, were injected bilaterally into the posterior dorsal pallium of pigeons. Three weeks after injection, we analyzed the expression of GFP on histological sections using confocal microscopy (Figure S1). We found that only rAAV2/7 resulted in robust GFP expression when injected into the dorsal pallium (Figure S1H). We therefore generated rAAV2/7 vectors driving the expression

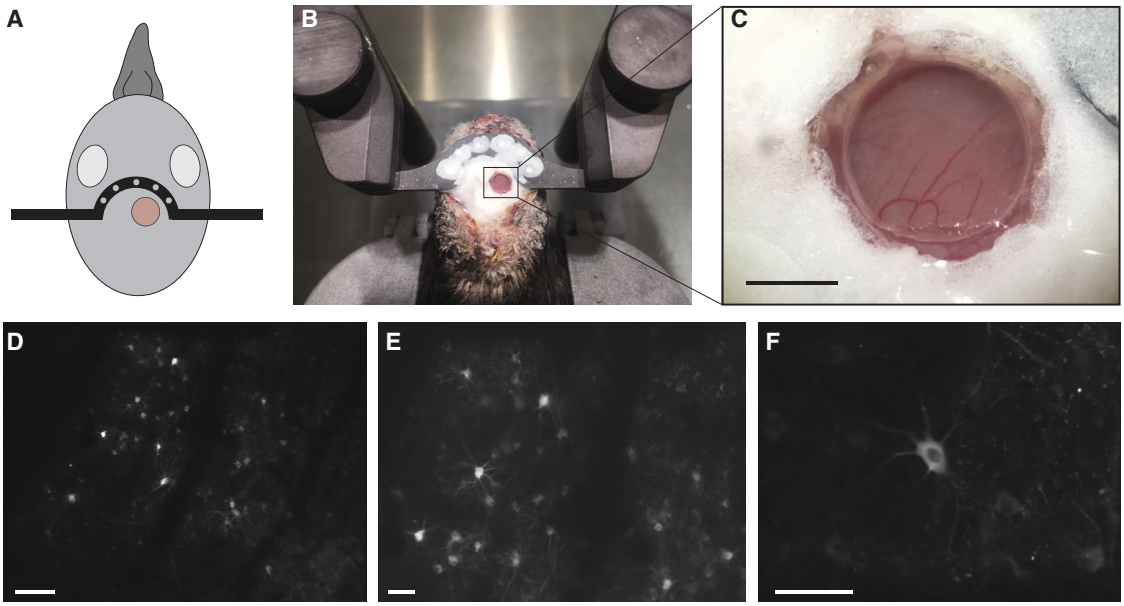

Figure 2. Optical window implantation for long-term *in vivo* 2-photon calcium imaging

(A and B) Top-down view on the pigeon head showing an implanted optical window (4 mm diameter) for 2-photon calcium imaging and a head bar attached to the skull to restrain the head under the microscope with 2 clamps.

(C) Zoom in on the optical window showing the brain surface and vasculature underneath the implanted window.

(D–F) Average intensity projections of imaging sessions acquired in resonant scanning mode showing that the system is capable of imaging large FOVs of up to 1 × 0.8 mm using low-magnification settings (D) and (E) and small FOVs focusing on single cells and individual dendrites using high-magnification settings (F). Scale bars: 2 mm in (C), 100 μm in (D), and 50 μm in (E) and (F).

See also Figures S3–S5 and Videos S1, S2, and S3.

of GCaMP6s under the CAG promoter. GCaMP6s was chosen because of its increased brightness, sensitivity, and signal-to-noise ratio.[32] We selected the CAG promoter because previous studies have demonstrated its high promoter activity in comparison to the CMV promoter in chicken fibroblasts.[33] Three weeks after injection, strong GCaMP6s expression was observed in the dorso-medial part of the hippocampus (Figure 1C). Next, we performed a double staining with the pan-neuronal marker NeuN and GFP to label GCaMP6s-positive neurons on sections prepared from injected birds (Figures 1D and 1E). Approximately 30% of NeuN-positive cells in the vicinity of the injection site (depth: ~500 μm) were GCaMP6s positive, revealing a high level of transduction efficiency (Figure 1F). All GCaMP6s-positive cells were NeuN positive (848 cells, n = 3 birds). Analysis of the GCaMP6s signal in the absence of GFP staining showed that it was enriched in somatic and dendritic compartments, with annular staining around the nucleus (Figures S2A–S2F). To test for a potential immune response to rAAV2/7-CAG-GCaMP6s injection, we stained with an antibody against GFAP, a commonly used marker for astrocytes.[34,35] We compared the mean fluorescent intensity of GFAP staining in the injected and non-injected hemispheres. We observed no significant difference in staining intensity ($p = 0.5112$, n = 3 birds), suggesting that rAAV2/7-CAG-GCaMP6s is well tolerated (Figure S2G–S2M). The number of DAPI-positive nuclei in the vicinity of the injection site was similar to the uninjected contralateral side, suggesting that rAAV2/7-CAG-GCaMP6s injection is not cytotoxic (Figure S2N; $p = 0.3232$, n = 3 birds). We did not observe any GCaMP6s-positive cells that were also GFAP positive (n = 3 birds), indicating a strong neuronal tropism of rAAV2/7 (Figure S2O). Together, these data show that rAAV2/7 can be used to effectively deliver calcium indicators such as GCaMP6s into neurons of the pigeon forebrain.

Optical window implantation for long-term 2-photon calcium imaging

To perform *in vivo* 2-photon calcium imaging experiments, optical access to the brain region of interest and a means to immobilize the head under the microscope are required. We therefore established surgical techniques to implant custom glass windows and head bars into the pigeon skull (Figures 2A–2C). Briefly, anesthetized birds were fixed in a stereotaxic apparatus, a round craniotomy (4 mm in diameter) was performed using a dental burr, and the dura and pia mater were carefully removed (Figures S3A and S3B). The latter was critical to prevent regrowth of brain membranes and to ensure that the cranial window remained clear for high-quality imaging over long time periods. Next, rAAV2/7-CAG-GCaMP6s was microinjected into the brain at volumes of ~200 nL and titers of $\sim 10^{12}$ GC/mL at depths ranging from 100 to 500 μm (Figure S3C). Windows were inserted into the craniotomy and positioned flush with the brain surface by applying light pressure before fixation to the skull using surgical glue and dental acrylic (Figures S3D and S3E). Finally, a custom head post made of polyetheretherketone was attached to the skull anterior of the window using dental acrylic to reversibly restrain the bird's head under the microscope objective (Figures 2A–2C and S3F).

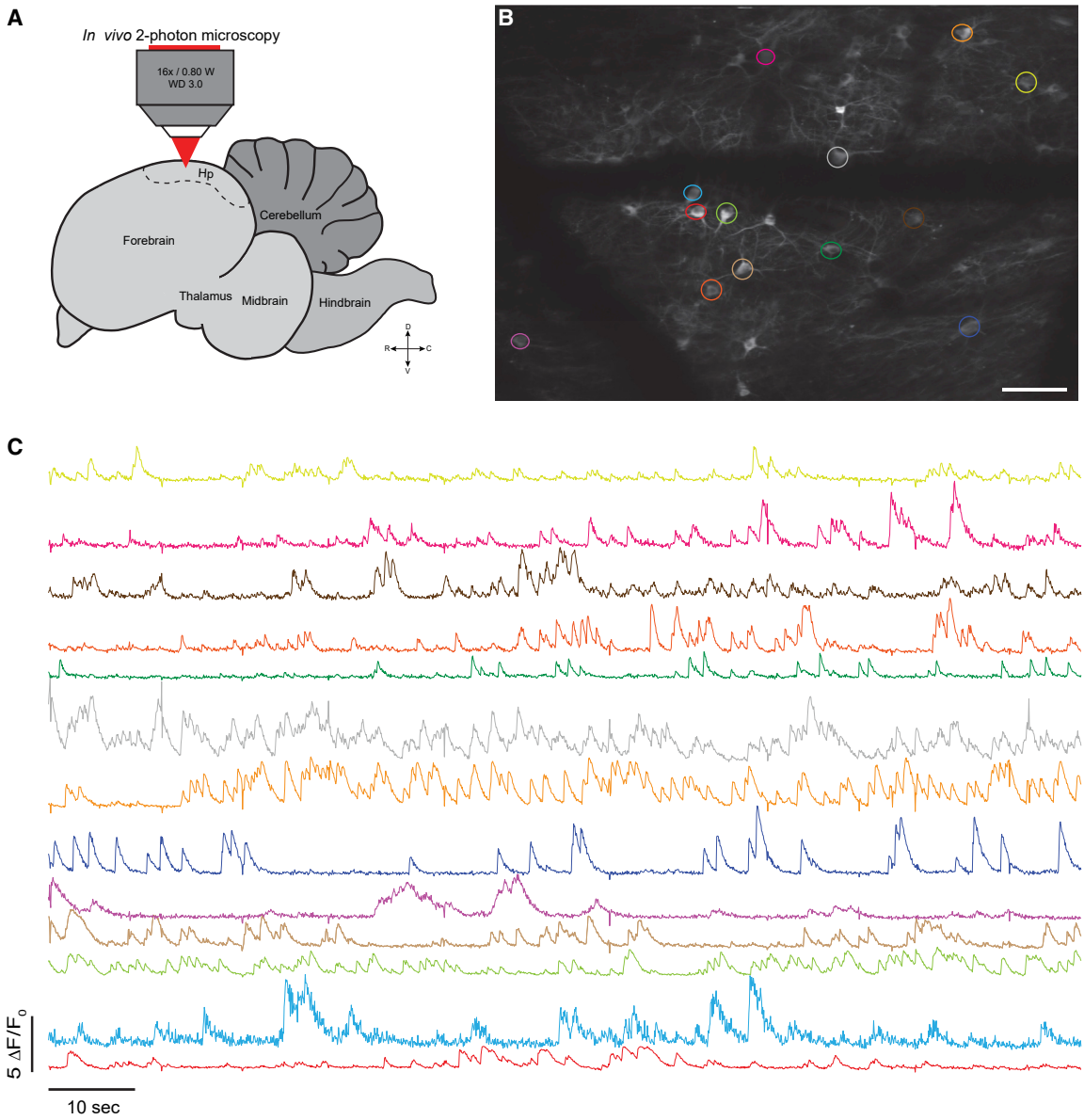

Figure 3. *In vivo* 2-photon calcium imaging in the hippocampus of awake pigeons

(A) *In vivo* 2-photon imaging of GCaMP6s-positive neurons in the awake pigeon hippocampus.

(B) Average intensity projection of an imaging session performed in darkness with no stimulation.

(C) Calcium dynamics of individual neurons ($\Delta F/F_0$). The colors correspond to the colored circles in (B).

Scale bar: 100 μm in (B).

See also Videos S1, S2, and S3.

In vivo 2-photon calcium imaging in the pigeon brain

We performed 2-photon imaging 3 weeks after surgery and delivery of GCaMP6s. Initial imaging revealed that we could obtain high-quality imaging with fields of view (FOVs) of up to 1 × 0.8 mm in the dorsal pallium at 1× magnification with 15.63 frames/s in resonant scanning mode (Figures 2D and 2E; Videos S1 and S2). Integrated high-magnification scan settings could be used to focus on single neurons and individual dendrites at micrometer resolution (8× magnification, 1 pixel ≈ 0.2 μm) (Figures 2F and S4; Video S3). The system enabled us to image neuronal populations up to ∼500 μm deep in the brain, covering large areas of the pigeon dorsal pallium including the dorso-posterior-located parts of the hippocampal formation, the laterally adjacent parahippocampal area (Figures 3A and 3B), and the dorso-anterior-located regions of the visual Wulst (hyperpallium apicale) (Figures 4A and 4B). After rigid alignment of the acquired frames using Scanbox software, individual neurons were manually segmented and average fluorescence intensities of each frame extracted. Background-subtracted calcium dynamics of

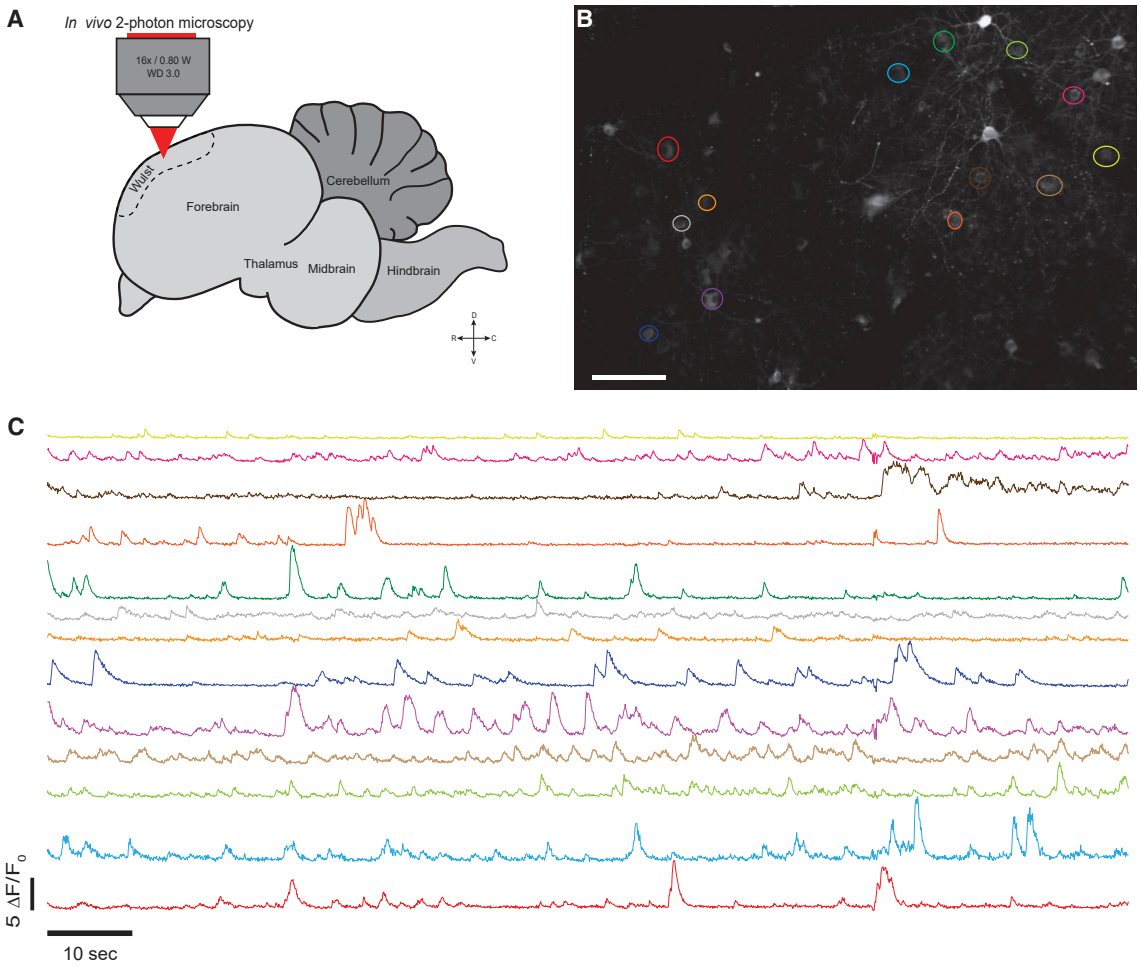

Figure 4. *In vivo* 2-photon calcium imaging in the visual Wulst of awake pigeons

(A) *In vivo* 2-photon imaging of GCaMP6s-positive neurons in the awake pigeon visual Wulst.

(B) Average intensity projection of an imaging session performed in darkness with no stimulation.

(C) Calcium dynamics of individual neurons ($\Delta F/F_0$). The colors correspond to the colored circles in (B).

Scale bar: 100 μm in (B).

See also Videos S1, S2, and S3.

individual neurons were computed as $\Delta F/F_0$. Initial imaging was performed in darkness and revealed a wide range of spontaneous activity, with some neurons displaying calcium transients very frequently and others infrequently (Figures 3C and 4C; Videos S1 and S2). The stable expression of GCaMP6s and the quality of the implanted windows made it possible to record the activity of neurons over long timescales. Strong GCaMP6s signals were observed 7 weeks after transduction (Figures S5A and S5B). In addition, we used the motion control system of our microscope to reliably track the activity of the same population of neurons over several days. Exemplarily, we recorded 31 neurons across 3 imaging sessions in the time course of 7 days (Figures S5C–S5F). Together, these results show that our 2-photon microscope system can be used to image calcium dynamics of dorsal pallial neurons in awake pigeons at single-cell and single-dendrite resolution over extended periods of time.

The neuronal correlates of color in the pigeon visual Wulst

To test the utility of our calcium imaging setup, we investigated the neuronal correlates of color vision in the pigeon visual Wulst. There are two ascending neuronal circuits that process visual information in birds: the (1) tectofugal and (2) thalamofugal pathways. The tectofugal pathway projects from the retina via the optic tectum to the thalamic nucleus rotundus and terminates in the entopallium.[36] In contrast, the thalamofugal pathway projects from the retina to the thalamic nucleus geniculatis lateralis pars dorsalis and terminates in a forebrain region called the visual Wulst. The Wulst is considered to be the functional equivalent of the mammalian primary visual cortex, but we do not understand how color is represented or encoded in this region.[37] To explore this, head-fixed pigeons expressing GCaMP6s in the visual Wulst were presented with whole-field color stimuli generated by an LED wall facing the pigeon (Figure 1A). The colors

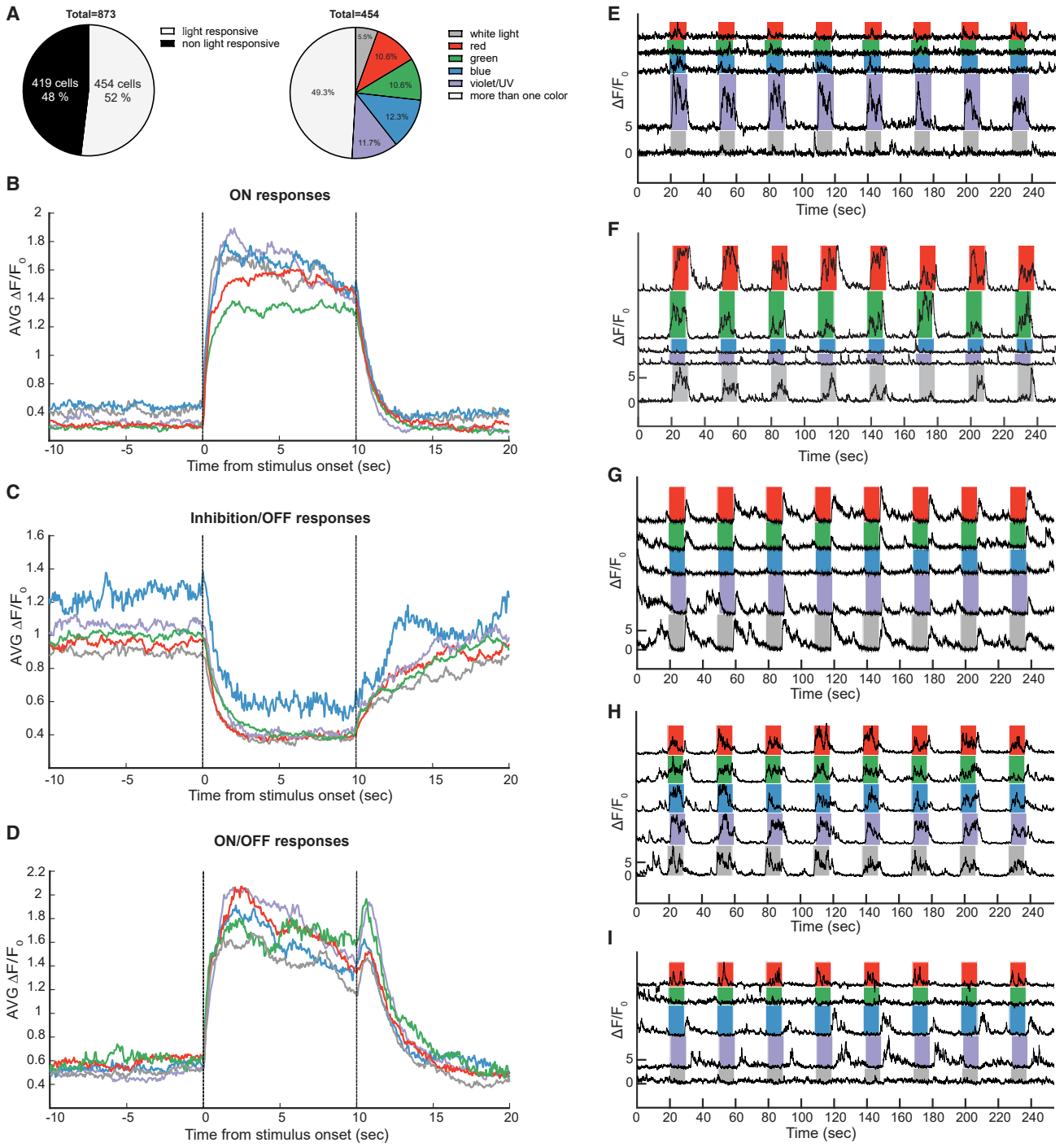

Figure 5. Light-driven responses in neurons of the pigeon visual Wulst

(A) Pie charts showing the percentages of cells that were responsive to light. In total, 873 cells were analyzed, out of which 454 (52%) were responsive to at least one light stimulus ($p < 0.05$, Kruskal-Wallis test with Dunn's correction). Out of those 454 responsive cells, 50.7% were selectively tuned to specific wavelengths (11.7% violet/UV, 12.3% blue, 10.6% green, 10.6% red, 5.5% white light), and 49.3% showed significant responses to more than one light stimulus.

(B–D) Characterization of population response profiles. Graphs display the average change of fluorescence (ΔF/F) for all ON (B), Inhibition/OFF (C), and ON/OFF (D) responses. 46% of responses were classified as ON, 38% as Inhibition/OFF, and 16% as ON/OFF.

(E) Example of an ON neuron that is selectively tuned to violet/UV light.

(F) Example of an ON neuron tuned to red and green light.

(legend continued on next page)

covered the range of wavelengths visible to the pigeon eye from UV/violet to red (Figure S6B).[38] The colors were presented for 10 s followed by 20 s of darkness (Figure S6A). We recorded responses from 873 neurons from 3 animals with 8–24 presentations of each color (a total of 26 FOVs with a mean of 33.6 neurons/FOV) (Figures 5A and S6A). After rigid alignment of the acquired frames, regions of interest (ROIs) were manually segmented, average fluorescence intensities for each frame extracted, $\Delta F/F_0$ computed, and fluorescent peaks detected. A fluorescent peak frequency for the 10 s before and during each color stimulus was calculated and compared using the Kruskal-Wallis test followed by Dunn's correction for multiple testing. Out of 873 neurons, 454 (52%) showed a significant increase or decrease of fluorescent peaks in response to at least one of the color stimuli. Out of those, 50.7% were most strongly tuned to single colors (11.7% violet/UV, 12.3% blue, 10.6% green, 10.6% red, 5.5% white light), and 49.3% were more broadly tuned to a range of colors (Figure 5A). On a population level, response profiles to any given light stimulus could be classified into three main groups: (1) ON responses showing an increase in fluorescent peak frequency during stimulation (46%; Figure 5B), (2) Inhibition/OFF responses showing a decrease in fluorescent peak frequency during stimulation followed by an increase at the offset of the stimuli (38%; Figure 5C), and (3) ON/OFF responses that were characterized by an increase of fluorescent peak frequency during stimulation and an additional transient offset response (16%; Figure 5D). Individual cells displayed diverse chromatic selectivities and response profiles (Figures 5E–5I). 39% of cells were exclusively ON responsive (Figures 5E and 5F), 42% were exclusively Inhibition/OFF responsive (Figure 5G), and 15% were responsive to the onset and offset (ON/OFF) of at least one chromatic stimulus (Figure 5H). Finally, a small percentage of cells (4%) displayed opponent responses to different colors (Figure 5I). Figure 5I shows an opponent cell that responds with an increase in activity (ON) when the bird was presented with red light and showed a decrease in activity at onset plus an increase at offset (Inhibition/OFF) when presented with blue and violet/UV stimuli. Collectively, these data demonstrate that our 2-photon imaging system is a useful tool to unravel sensory coding in the pigeon brain.

DISCUSSION

In this article, we report the implementation of a *in vivo* 2-photon calcium imaging system for awake, head-restrained pigeons. Our system allows long-term imaging of large numbers of neurons in different regions of the pigeon dorsal forebrain with single-cell resolution. High-quality cranial window preparations (Figures 2 and S3) and stable GCaMP6s expression (Figure 1) made it possible to track the activity of individual neurons over several days (Figures S5C–S5F) and to image different neuronal cell populations over weeks in the same bird (Figures S5A and S5B). These advancements open up the possibility for future studies investigating representational drift in visual brain regions and the formation and recall of episodic memory in the hippocampus.[39–41] Furthermore, with optogenetic methods now established in pigeons, it is entirely possible to combine our calcium imaging approach with manipulation of neural circuits through optical stimulation using rAAV2/7-mediated delivery of optogenetic actuators.[29,42] Our system could also be used for operant conditioning paradigms to investigate neural activity during cognitive tasks, as it has been shown that mandibulations can be employed as a readout when using head-fixed pigeons.[19] A recent study has reported that AAV1 is an efficient vector for viral gene delivery in the pigeon brain,[29] whereas we did not observe GFP-positive neurons when using AAV1 (Figure S2). One explanation for this result could be the different genetic backgrounds. It has been shown that the genetic background of mice has a strong influence on the tropism and transduction rates of AAVs in the murine brain.[43]

To test if our 2-photon microscopy setup can be used to study sensory processing, we investigated how color information is processed and represented in the pigeon visual Wulst. Overall, light-responsive neurons could be classified into 4 groups: cells that responded with increased activity at the onset of stimuli (ON cells; Figures 5E and 5F), cells that responded with a decrease in activity during the stimuli followed by an increase at the offset (Inhibition/OFF cells; Figure 5G), a smaller group of cells that displayed dual responses (ON/OFF cells; Figure 5H), and, in rare cases, cells that displayed opponent responses to different chromatic stimuli (Figure 5I). We identified an approximately balanced number of neurons that selectively respond to specific colors but also a large number of neurons that displayed preferences to more than one or, in some cases, all colors (Figures 5A and 5E–5I). These findings lend support to genetic, molecular, and behavioral studies showing that pigeons have 4 color-sensitive cone types, enabling tetrachromatic color vision that extends to the UV range.[44–46]

While there is a wealth of behavioral data highlighting the importance of color vision in birds, and while the first large-scale functional interrogation of the *ex vivo* avian retina was recently published,[47,48] we lack a detailed understanding of how color is processed in the bird brain at an ensemble and a single-cell level. Using extracellular recording techniques, luminance-sensitive, color-selective, and color-opponent neurons have been identified in the nucleus rotundus, the thalamic relay station of the tectofugal pathway.[49–51] Local field potentials (LFPs) in response to full-field color stimuli have been recorded from several regions of the visual system, including the visual Wulst in anesthetized zebra finches.[52] These experiments revealed distinct LFPs in all analyzed areas, with the strongest responses to colors in the blue-green spectrum. To our knowledge, the experiments presented in this study are the first to explore color processing in the avian visual Wulst on a single-cell level using calcium imaging, highlighting the power of this technology and the opportunities for new discoveries in avian sensory and cognitive biology. In the future, this approach will permit the analysis of large numbers of neurons within the visual Wulst

(G) Example of a neuron displaying Inhibition/OFF responses to all chromatic stimuli.
(H) Example of a neuron displaying ON/OFF responses to all chromatic stimuli.
(I) Example of a neuron displaying color-opponent responses showing ON responses to red stimuli and Inhibition/OFF responses to blue and violet/UV stimuli. Calcium dynamics of individual cells are shown as $\Delta F/F_0$.

and the longitudinal tracking of these cells over time. Given the evidence for a light-dependent magnetic compass in birds, which is dependent on blue-green light and on the integrity of a region of the visual Wulst (Cluster N),[53,54] it will be particularly interesting to use this technology to understand how magnetic information is encoded in the avian brain.

Limitations of the study

At present, our setup is restricted to imaging superficial regions of the dorsal forebrain. We expect, however, that the attachment of microprisms to the bottom of the cranial glass windows or the injection of red-shifted calcium indicators will permit imaging in deeper regions.[55–57] Currently, we are using a pan-neuronal, cell-type-unspecific promoter to achieve high expression levels. Some experiments might necessitate the visualization of specific cell types. Driving transgene expression in a cell-type-specific manner could be achieved using different promoters or by utilizing a targeted retrograde-labeling approach.[31]

STAR★METHODS

Detailed methods are provided in the online version of this paper and include the following:

- KEY RESOURCES TABLE
- RESOURCE AVAILABILITY
  - Lead contact
  - Materials availability
  - Data and code availability
- EXPERIMENTAL MODEL AND SUBJECT DETAILS
- METHOD DETAILS
  - Transduction efficiency of AAV serotypes in the pigeon brain
  - rAAV2/7-CAG-GCaMP6s virus production
  - Glass window preparation
  - Cranial window surgery and AAV injection for GCaMP6s expression
  - Viral transduction and GCaMP6s expression
  - Assessing immune response to rAAV2/7-CAG-GCaMP6s injection
  - 2-Photon microscopy
  - Light stimulation
- QUANTIFICATION AND STATISTICAL ANALYSIS

SUPPLEMENTAL INFORMATION

Supplemental information can be found online at https://doi.org/10.1016/j.crmeth.2024.100711.

ACKNOWLEDGMENTS

D.A.K. is supported by the European Research Council (ERC Consolidator Grant; 819336). We wish to thank Neurolabware, Martin Colombini, and colleagues from the IMP workshop for their assistance in building the 2-photon microscope.

AUTHOR CONTRIBUTIONS

Conceptualization, S.N. and D.A.K.; investigation, S.N.; formal analysis, S.N., G.C.N., and H.S.K.; writing – original draft, S.N. and D.A.K.; writing – review & editing, S.N., D.A.K., H.S.K., G.C.N., and T.C.; funding acquisition, D.A.K.; supervision, D.A.K.

DECLARATION OF INTERESTS

The authors declare no competing interests.

Received: June 10, 2023
Revised: November 5, 2023
Accepted: January 26, 2024
Published: February 20, 2024

REFERENCES

1. Nieder, A., Wagener, L., and Rinnert, P. (2020). A neural correlate of sensory consciousness in a corvid bird. Science *369*, 1626–1629. https://doi.org/10.1126/science.abb1447.
2. Ben-Yisahay, E., Krivoruchko, K., Ron, S., Ulanovsky, N., Derdikman, D., and Gutfreund, Y. (2021). Directional tuning in the hippocampal formation of birds. Curr. Biol. *31*, 2592–2602.e2594. https://doi.org/10.1016/j.cub.2021.04.029.
3. Payne, H.L., Lynch, G.F., and Aronov, D. (2021). Neural representations of space in the hippocampus of a food-caching bird. Science *373*, 343–348. https://doi.org/10.1126/science.abg2009.
4. Clark, W.J., and Colombo, M. (2020). The functional architecture, receptive field characteristics, and representation of objects in the visual network of the pigeon brain. Prog. Neurobiol. *195*, 101781. https://doi.org/10.1016/j.pneurobio.2020.101781.
5. Levenson, R.M., Krupinski, E.A., Navarro, V.M., and Wasserman, E.A. (2015). Pigeons (Columba livia) as trainable observers of pathology and radiology breast cancer images. PLoS One *10*, e0141357.
6. Ghosh, N., Lea, S.E.G., and Noury, M. (2004). Transfer to intermediate forms following concept discrimination by pigeons: chimeras and morphs. J. Exp. Anal. Behav. *82*, 125–141. https://doi.org/10.1901/jeab.2004.82-125.
7. von Fersen, L., and Delius, J.D. (1989). Long-term retention of many visual patterns by pigeons. Ethology *82*, 141–155. https://doi.org/10.1111/j.1439-0310.1989.tb00495.x.
8. Fabricius, E., and Jansson, A.-M. (1963). Laboratory observations on the reproductive behaviour of the pigeon (Columba livia) during the pre-incubation phase of the breeding cycle. Anim. Behav. *11*, 534–547. https://doi.org/10.1016/0003-3472(63)90276-8.
9. Emmerton, J., and Remy, M. (1983). The pigeon's sensitivity to ultraviolet and 'visible'light. Experientia *39*, 1161–1163. https://doi.org/10.1007/BF01943162.
10. Kreithen, M.L., and Quine, D.B. (1979). Infrasound detection by the homing pigeon: a behavioral audiogram. J. Comp. Physiol. *129*, 1–4. https://doi.org/10.1007/BF00679906.
11. Mora, C.V., Acerbi, M.L., and Bingman, V.P. (2014). Conditioned discrimination of magnetic inclination in a spatial-orientation arena task by homing pigeons (Columba livia). J. Exp. Biol. *217*, 4123–4131. https://doi.org/10.1242/jeb.101113.
12. Güntürkün, O., and Bugnyar, T. (2016). Cognition without cortex. Trends Cogn. Sci. *20*, 291–303. https://doi.org/10.1901/jeab.2004.82-125.
13. Clayton, N.S., and Emery, N.J. (2015). Avian models for human cognitive neuroscience: a proposal. Neuron *86*, 1330–1342. https://doi.org/10.1016/j.neuron.2015.04.024.
14. Ng, B.S.W., Grabska-Barwińska, A., Güntürkün, O., and Jancke, D. (2010). Dominant vertical orientation processing without clustered maps: early visual brain dynamics imaged with voltage-sensitive dye in the pigeon visual Wulst. J. Neurosci. *30*, 6713–6725. https://doi.org/10.1523/JNEUROSCI.4078-09.2010.

15. Keary, N., Voss, J., Lehmann, K., Bischof, H.J., and Löwel, S. (2010). Optical imaging of retinotopic maps in a small songbird, the zebra finch. PLoS One *5*, e11912. https://doi.org/10.1371/journal.pone.0011912.

16. Bischof, H.-J., Eckmeier, D., Keary, N., Löwel, S., Mayer, U., and Michael, N. (2016). Multiple Visual Field Representations in the Visual Wulst of a Laterally Eyed Bird, the Zebra Finch (Taeniopygia guttata). PLoS One *11*, e0154927. https://doi.org/10.1371/journal.pone.0154927.

17. Michael, N., Bischof, H.-J., and Löwel, S. (2014). Flavoprotein autofluorescence imaging of visual system activity in zebra finches and mice. PLoS One *9*, e85225. https://doi.org/10.1371/journal.pone.0085225.

18. Liu, G.B., and Pettigrew, J.D. (2003). Orientation mosaic in barn owl's visual Wulst revealed by optical imaging: comparison with cat and monkey striate and extra-striate areas. Brain Res. *961*, 153–158. https://doi.org/10.1016/S0006-8993(02)03747-2.

19. Behroozi, M., Helluy, X., Ströckens, F., Gao, M., Pusch, R., Tabrik, S., Tegenthoff, M., Otto, T., Axmacher, N., Kumsta, R., et al. (2020). Event-related functional MRI of awake behaving pigeons at 7T. Nat. Commun. *11*, 4715–4812. https://doi.org/10.1038/s41467-020-18437-1.

20. Picardo, M.A., Merel, J., Katlowitz, K.A., Vallentin, D., Okobi, D.E., Benezra, S.E., Clary, R.C., Pnevmatikakis, E.A., Paninski, L., and Long, M.A. (2016). Population-level representation of a temporal sequence underlying song production in the zebra finch. Neuron *90*, 866–876. https://doi.org/10.1016/j.neuron.2016.02.016.

21. Katlowitz, K.A., Picardo, M.A., and Long, M.A. (2018). Stable sequential activity underlying the maintenance of a precisely executed skilled behavior. Neuron *98*, 1133–1140.e3. https://doi.org/10.1016/j.neuron.2018.05.017.

22. Moll, F.W., Kranz, D., Corredera Asensio, A., Elmaleh, M., Ackert-Smith, L.A., and Long, M.A. (2023). Thalamus drives vocal onsets in the zebra finch courtship song. Nature *616*, 132–136. https://doi.org/10.1038/s41586-023-05818-x.

23. Güntürkün, O., Stüttgen, M., and Manns, M. (2014). Pigeons as a model species for cognitive neuroscience. e-Neuroforum *5*, 86–92. https://doi.org/10.1007/s13295-014-0057-5.

24. Güntürkün, O., Ströckens, F., Scarf, D., and Colombo, M. (2017). Apes, feathered apes, and pigeons: differences and similarities. Current Opinion in Behavioral Sciences *16*, 35–40. https://doi.org/10.1016/j.cobeha.2017.03.003.

25. Aschauer, D.F., Kreuz, S., and Rumpel, S. (2013). Analysis of Transduction Efficiency, Tropism and Axonal Transport of AAV Serotypes 1, 2, 5, 6, 8 and 9 in the Mouse Brain. PLoS One *8*, e76310. https://doi.org/10.1371/journal.pone.0076310.

26. Zincarelli, C., Soltys, S., Rengo, G., and Rabinowitz, J.E. (2008). Analysis of AAV serotypes 1–9 mediated gene expression and tropism in mice after systemic injection. Mol. Ther. *16*, 1073–1080. https://doi.org/10.1038/mt.2008.76.

27. Tenenbaum, L., Chtarto, A., Lehtonen, E., Velu, T., Brotchi, J., and Levivier, M. (2004). Recombinant AAV-mediated gene delivery to the central nervous system. J. Gene Med. *6*, S212–S222. https://doi.org/10.1002/jgm.506.

28. McFarland, N.R., Lee, J.-S., Hyman, B.T., and McLean, P.J. (2009). Comparison of transduction efficiency of recombinant AAV serotypes 1, 2, 5, and 8 in the rat nigrostriatal system. J. Neurochem. *109*, 838–845. https://doi.org/10.1111/j.1471-4159.2009.06010.x.

29. Rook, N., Tuff, J.M., Isparta, S., Masseck, O.A., Herlitze, S., Güntürkün, O., and Pusch, R. (2021). AAV1 is the optimal viral vector for optogenetic experiments in pigeons (Columba livia). Commun. Biol. *4*, 100–116. https://doi.org/10.1038/s42003-020-01595-9.

30. Ahmadiantehrani, S., and London, S.E. (2017). A reliable and flexible gene manipulation strategy in posthatch zebra finch brain. Sci. Rep. *7*, 43244. https://doi.org/10.1038/srep43244.

31. Düring, D.N., Dittrich, F., Rocha, M.D., Tachibana, R.O., Mori, C., Okanoya, K., Boehringer, R., Ehret, B., Grewe, B.F., Gerber, S., et al. (2020). Fast retrograde access to projection neuron circuits underlying vocal learning in songbirds. Cell Rep. *33*, 108364. https://doi.org/10.1016/j.celrep.2020.108364.

32. Chen, T.-W., Wardill, T.J., Sun, Y., Pulver, S.R., Renninger, S.L., Baohan, A., Schreiter, E.R., Kerr, R.A., Orger, M.B., Jayaraman, V., et al. (2013). Ultrasensitive fluorescent proteins for imaging neuronal activity. Nature *499*, 295–300. https://doi.org/10.1038/nature12354.

33. Seo, H.W., Kim, T.M., Choi, J.W., Han, B.K., Song, G., and Han, J.Y. (2010). Evaluation of combinatorial cis-regulatory elements for stable gene expression in chicken cells. BMC Biotechnol. *10*, 69. https://doi.org/10.1186/1472-6750-10-69.

34. Rook, N., Stacho, M., Schwarz, A., Bingman, V.P., and Güntürkün, O. (2023). Neuronal circuits within the homing pigeon hippocampal formation. J. Comp. Neurol. *531*, 790–813. https://doi.org/10.1002/cne.25462.

35. Sievers, J., Hartmann, D., Pehlemann, F.W., and Berry, M. (1992). Development of astroglial cells in the proliferative matrices, the granule cell layer, and the hippocampal fissure of the hamster dentate gyrus. J. Comp. Neurol. *320*, 1–32. https://doi.org/10.1002/cne.903200102.

36. Karten, H., and Nauta, W. (1968). Organization of Retinothalamic Projections in Pigeon and Owl. In 2 (Wiley-Liss Div John Wiley & Sons Inc), p. 373.

37. Shimizu, T., Patton, T.B., and Husband, S.A. (2010). Avian visual behavior and the organization of the telencephalon. Brain Behav. Evol. *75*, 204–217. https://doi.org/10.1159/000314283.

38. Vorobyev, M., Osorio, D., Bennett, A.T., Marshall, N.J., and Cuthill, I.C. (1998). Tetrachromacy, oil droplets and bird plumage colours. J. Comp. Physiol. *183*, 621–633. https://doi.org/10.1007/s003590050286.

39. Deitch, D., Rubin, A., and Ziv, Y. (2021). Representational drift in the mouse visual cortex. Curr. Biol. *31*, 4327–4339.e6. https://doi.org/10.1016/j.cub.2021.07.062.

40. Rolls, E.T. (2018). The storage and recall of memories in the hippocampo-cortical system. Cell Tissue Res. *373*, 577–604. https://doi.org/10.1007/s00441-017-2744-3.

41. Izquierdo, I., and Medina, J.H. (1997). Memory formation: the sequence of biochemical events in the hippocampus and its connection to activity in other brain structures. Neurobiol. Learn. Mem. *68*, 285–316. https://doi.org/10.1006/nlme.1997.3799.

42. Russell, L.E., Dalgleish, H.W.P., Nutbrown, R., Gauld, O.M., Herrmann, D., Fişek, M., Packer, A.M., and Häusser, M. (2022). All-optical interrogation of neural circuits in behaving mice. Nat. Protoc. *17*, 1579–1620. https://doi.org/10.1038/s41596-022-00691-w.

43. He, T., Itano, M.S., Earley, L.F., Hall, N.E., Riddick, N., Samulski, R.J., and Li, C. (2019). The Influence of Murine Genetic Background in Adeno-Associated Virus Transduction of the Mouse Brain. Hum. Gene Ther. Clin. Dev. *30*, 169–181. https://doi.org/10.1089/humc.2019.030.

44. Palacios, A.G., and Varela, F.J. (1992). Color mixing in the pigeon (Columba livia) II: A psychophysical determination in the middle, short and near-UV wavelength range. Vision Res. *32*, 1947–1953. https://doi.org/10.1016/0042-6989(92)90054-M.

45. Kawamura, S., Blow, N.S., and Yokoyama, S. (1999). Genetic analyses of visual pigments of the pigeon (Columba livia). Genetics *153*, 1839–1850. https://doi.org/10.1093/genetics/153.4.1839.

46. Palacios, A., Martinoya, C., Bloch, S., and Varela, F.J. (1990). Color mixing in the pigeon: A psychophysical determination in the longwave spectral range. Vision Res. *30*, 587–596. https://doi.org/10.1016/0042-6989(92)90054-M.

47. Kelber, A. (2019). Bird colour vision–from cones to perception. Current Opinion in Behavioral Sciences *30*, 34–40. https://doi.org/10.1016/j.cobeha.2019.05.003.

48. Seifert, M., Roberts, P.A., Kafetzis, G., Osorio, D., and Baden, T. (2023). Birds multiplex spectral and temporal visual information via retinal On- and Off-channels. Nat. Commun. *14*, 5308. https://doi.org/10.1038/s41467-023-41032-z.

49. Wang, Y.-C., Jiang, S., and Frost, B.J. (1993). Visual processing in pigeon nucleus rotundus: luminance, color, motion, and looming subdivisions. Vis. Neurosci. *10*, 21–30. https://doi.org/10.1017/s0952523800003199.

50. Granda, A.M., and Yazulla, S. (1971). The spectral sensitivity of single units in the nucleus rotundus of pigeon, Columba livia. J. Gen. Physiol. *57*, 363–384. https://doi.org/10.1085/jgp.57.3.363.

51. Yazulla, S., and Granda, A.M. (1973). Opponent-color units in the thalamus of the pigeon (Columba livia). Vision Res. *13*, 1555–1563. https://doi.org/10.1016/0042-6989(73)90014-x.

52. Hsiao, Y.-T., Chen, T.-C., Yu, P.-H., Huang, D.-S., Hu, F.-R., Chuong, C.-M., and Chang, F.-C. (2020). Connectivity between nidopallium caudolateral and visual pathways in color perception of zebra finches. Sci. Rep. *10*, 19382. https://doi.org/10.1038/s41598-020-76542-z.

53. Zapka, M., Heyers, D., Hein, C.M., Engels, S., Schneider, N.L., Hans, J., Weiler, S., Dreyer, D., Kishkinev, D., Wild, J.M., and Mouritsen, H. (2009). Visual but not trigeminal mediation of magnetic compass information in a migratory bird. Nature *461*, 1274–1277. https://doi.org/10.1038/nature08528.

54. Wiltschko, W., and Wiltschko, R. (1995). Migratory orientation of European Robins is affected by the wavelength of light as well as by a magnetic pulse. J. Comp. Physiol. *177*, 363–369. https://doi.org/10.1007/BF00192425.

55. Andermann, M.L., Gilfoy, N.B., Goldey, G.J., Sachdev, R.N.S., Wölfel, M., McCormick, D.A., Reid, R.C., and Levene, M.J. (2013). Chronic cellular imaging of entire cortical columns in awake mice using microprisms. Neuron *80*, 900–913. https://doi.org/10.1016/j.neuron.2013.07.052.

56. Goldey, G.J., Roumis, D.K., Glickfeld, L.L., Kerlin, A.M., Reid, R.C., Bonin, V., Schafer, D.P., and Andermann, M.L. (2014). Removable cranial windows for long-term imaging in awake mice. Nat. Protoc. *9*, 2515–2538. https://doi.org/10.1038/nprot.2014.165.

57. Hussein, W., and Berlin, S. (2020). Red photoactivatable genetic optical-indicators. Front. Cell. Neurosci. *14*, 113. https://doi.org/10.3389/fncel.2020.00113.

58. Schindelin, J., Arganda-Carreras, I., Frise, E., Kaynig, V., Longair, M., Pietzsch, T., Preibisch, S., Rueden, C., Saalfeld, S., Schmid, B., et al. (2012). Fiji: an open-source platform for biological-image analysis. Nat. Methods *9*, 676–682. https://doi.org/10.1038/nmeth.2019.

STAR★METHODS

KEY RESOURCES TABLE

REAGENT or RESOURCE	SOURCE	IDENTIFIER
Antibodies		
anti-GFP	Abcam	Cat#ab6556; RRID: AB_305564
anti-NeuN	Millipore	Cat#Mab377; RRID:AB_2298772
Anti-GFAP	Invitrogen	Cat#13-0300; RRID: AB_2532994
Alexa Fluor 488 anti-rabbit	Thermo Fisher	Cat#A-21206; RRID: AB_2535792
Alexa Fluor 568 anti-mouse	Thermo Fisher	Cat#A10037; RRID: AB_2534013
Alexa Fluor 568 anti-rat	Thermo Fisher	Cat#A11077; RRID: AB_2534121
Bacterial and virus strains		
pAAV.CAG.GCaMP6s.WPRE.SV40	Chen et al.[32]	Addgene Cat#100844
pAAV2.7	Addgene	Cat#112863
pAdDeltaF6	Addgene	Cat#112867
rAAV2/7-CAG-GCaMP6s	This paper	N/A
Chemicals, peptides, and recombinant proteins		
Paraformaldehyde	Sigma Aldrich	Cat#158127
Triton X-100	Sigma Aldrich	Cat#T8787
Donkey serum	Abcam	Cat# ab7475
Fluorescent Mounting Medium	Dako	Cat#S302380
PEI Max 40K	Polysciences	Cat#24765
Sucrose	Sigma Aldrich	Cat#S9378
Optiprep	Sigma-Aldrich	Cat#D1556
Fluorescent mounting medium	Dako	Cat#S302380
Critical commercial assays		
AAV Serotype Blast Kit	Applied Biological Materials Inc.	Cat#AAV099
Amicon Ultra-15 100K columns	Merck	Cat#UFC910008
SsoAdvance Universal SYBR Green Supermix	Bio-Rad	Cat#1725271
Experimental models: Organisms/strains		
Pigeon (*Columba livia*)		N/A
Oligonucleotides		
GCaMP6s_1_F: ATGAAATACAGGGACACGGAAGAA	This paper	N/A
GCaMP6s_1_R: ACTTCTCTCCAAGGTTTGTCATCA	This paper	N/A
Software and algorithms		
FIJI	Schindelin et al.[58]	https://imagej.net/software/fiji/
Prism software	GraphPad Software	N/A
MATLAB	The MathWorks Inc.	N/A
Scanbox Software	Neurolabware	N/A
Other		
Cover glasses (4 mm, 5mm)	Warner Instruments	Cat#64–0724, Cat#64-0700
Optical adhesive	Norland Products	Cat#106
Surgical drill	Foredom Electric Company	Cat#51449
Heating blanket	Harvard Apparatus	Cat#K024520)
Stereotaxic apparatus	Kopf Instruments	Cat#900LS
Kwick-Cast silicone sealant	World Precision Instruments	Cat#KWIK-CAST
Surgical glue	Trusetal	Cat#B031232971B
2-photon microscope	Neurolabware	N/A

(*Continued on next page*)

Continued

REAGENT or RESOURCE	SOURCE	IDENTIFIER
2-photon laser	Coherent	#GDP.1185894.8031
Femtojet microinjection system	Eppendorf	Cat#5247
3D printed body harness	This paper	https://github.com/KeaysLab/DesignFiles https://doi.org/10.5281/zenodo.10556243
Head clamps	This paper	https://github.com/KeaysLab/DesignFiles https://doi.org/10.5281/zenodo.10556243
Head post	This paper	https://github.com/KeaysLab/DesignFiles https://doi.org/10.5281/zenodo.10556243

RESOURCE AVAILABILITY

Lead contact

Further information and requests for reagents may be directed to and will be fulfilled by the lead contact: David A. Keays (keays@biologie.uni-muenchen.de).

Materials availability

Commercially available reagents are listed in the key resources table. The rAAV2/7-CAG-GCaMP6s virus is available upon request.

Data and code availability

- Data generated in this study are available from the lead contact without restriction. Design files of the pigeon stage are available from the Keays Lab Github repository (https://github.com/KeaysLab/DesignFiles). An archival DOI is listed in the key resources table.
- This study does not report original code.
- Any additional information required to re-analyze the data reported in this paper are available from the lead contact upon request.

EXPERIMENTAL MODEL AND SUBJECT DETAILS

Pigeons (*Columba livia*) at ~1 year of age were maintained on a 12:12 light-dark cycle at 21°C in a custom-built aviary. Three female birds were used for the color exposure experiments. Experimental procedures were performed in accordance with an ethical framework granted by the city of Vienna (Magistratsabteilung 58, GZ: 659507/2017/1) and the Regierung of Oberbayern (ROB-55.2-2532.Vet_02-21-86).

METHOD DETAILS

Transduction efficiency of AAV serotypes in the pigeon brain

Pigeons were anesthetized using 0.1 mL/kg of ketamine (AniMedica, Ketasol, #6680117) and 0.1 mL/kg of metedomidinhydrochlorid (Orion Corporation, Domitor, #107118-9), placed on a heating blanket set to 40°C (Harvard Apparatus, #K024520) and fixed in a stereotaxic apparatus (Kopf Instruments, #900LS). The skin above the skull was protracted and a small craniotomy performed using a dental burr. To screen for the optimal adeno-associated virus for transgene expression in the pigeon forebrain, serotypes AAV1-9, harboring the genetic sequence of GFP under the CMV promoter (Applied Biological Materials Inc., AAV Serotype Blast Kit, #AAV099), were injected bilaterally into the dorsal forebrain (1 serotype/pigeon, A +5.50, L +/−2, ~5 injections/bird/hemisphere, volume: ~200 nL, titer: 10^{11} GC/mL). The craniotomy was sealed with Kwick-Cast and the skin was retracted and glued together with surgical glue. Anesthesia was antagonized with 0.1 mL/kg atipamezolhydrochlorid (Orion Corporation, Antisedan, #107185-9) and pigeons were administered butorphanol (2 mg/kg) (Richter Pharma AG, Butomidor #0217165AG) and meloxicam (0.5 mg/kg) (Böhringer Ingelheim, Metacam, #K21001B-57) for 3 days post-surgery for analgesia. 3 weeks after injections, the birds were transcardially perfused with 200 mL of PBS and 200 mL of 4% PFA (Sigma Aldrich, 158127), the brains were dissected, post-fixed overnight in 4% PFA and dehydrated in 30% sucrose (Sigma Aldrich, S9378). Brains were sliced in the coronal plane on a microtome (40 μm sections). The slides were incubated with primary antibody anti-GFP (Abcam, ab6556, conc: 1:500) diluted in 0.3% Triton X-100 (Sigma-Aldrich, T8787) supplemented with 2% donkey serum (Abcam, ab7475) for 10 h at 4°C, incubated with secondary antibodies Alexa Fluor 488 anti-rabbit (Thermo Fisher, A-21206), counterstained with DAPI and imaged using a confocal microscope (Zeiss, LSM 700).

rAAV2/7-CAG-GCaMP6s virus production

Lenti-X Hek293T cells cultured in DMEM supplemented with 10% FCS, 1% Penicillin/Streptomycin and 1% Sodiumpyruvate were transfected with 0.5 mg of pAAV.CAG.GCaMP6s.WPRE.SV40 (Addgene, #100844), pAAV2.7 (Addgene, #112863) and pAdDeltaF6 (Addgene, #112867) plasmids each by PEI transfection method (PEI Max 40K, Polysciences, #24765). 5 days after transfection cells were harvested, pelleted, resuspended in lysis buffer (150 mM NaCl, 20 mM Tris) and lysed using repeated freeze thaw cycles (3x, 15 min 37°C, 15 min dry ice). $MgCl_2$ and Benzonase (Molecular Biology Facility, IMP Vienna) was added to the cell lysates in a final concentration of 1 mM and 250U/ml respectively and incubated for 15 min at 37°C before dounce homogenization. Viral particles were then purified using Iodixanol gradient (Optiprep, Sigma-Aldrich, #D1556) centrifugation at 62000 rpm for 140 min. Virus was collected from the 40% Iodixanol fraction and concentrated by centrifugation (30 min, 3500 rpm) using Amicon Ultra-15 100K columns (Merck, #UFC910008). Viral titer was determined by qPCR using a Bio-Rad CFX Connect cycler (Bio-Rad, Hercules, CA, USA, 1855201) and SsoAdvance Universal SYBR Green Supermix (Bio-Rad, #1725271) (primers: GCaMP6s_1_F ATGAAATACA GGGACACGGAAGAA; GCaMP6s_1_R ACTTCTCTCCAAGGTTTGTCATCA).

Glass window preparation

Layered windows were prepared by attaching three 4 mm round cover glasses (Warner Instruments, 64–0724) and one 5 mm round cover glass (Warner Instruments, 64–0700) using optical adhesive (Norland Products, 7106) and UV light. A detailed protocol can be found in Goldey et al..[56]

Cranial window surgery and AAV injection for GCaMP6s expression

Pigeons were anesthetized using 0.1 mL/kg of ketamine (AniMedica, Ketasol, #6680117) and 0.1 mL/kg of metedomidinhydrochlorid (Orion Corporation, Domitor, #107118-9), placed on a heating blanket set to 40°C (Harvard Apparatus, #K024520) and fixed in a stereotaxic apparatus (Kopf Instruments, #900LS). The skin above the skull was protracted and a round craniotomy (4 mm diameter) centered around the medial hippocampal formation (A +5.50, L +/−2) or the visual wulst (A +11.50, L+2) was performed using a surgical drill (Foredom Electric Company, #51449). The dura was removed and rAAV2/7-CAG-GCaMP6s was pressure injected (~5 injections/bird, volume: ~200 nL, titer: $2.4x10^{12}$ GC/ml) using a microinjector (Eppendorf, Femtojet #5247) equipped with a glass microcapillary. A glass window was placed onto the craniotomy and fixed to the bone with surgical glue (Trusetal, TRUglue #B031232971B) and dental acrylic (Lang Dental, #1402X6, #1410). A custom head bar made of polyetheretherketon (PEEK) was attached to the skull with dental acrylic and the skin was retracted and glued together with surgical glue. Anesthesia was antagonized with 0.1 mL/kg atipamezolhydrochlorid (Orion Corporation, Antisedan, #107185-9) and pigeons were administered butorphanol (2 mg/kg) (Richter Pharma AG, Butomidor #0217165AG) and meloxicam (0.5 mg/kg) (Böhringer Ingelheim, Metacam, #K21001B-57) for 3 days post-surgery for analgesia.

Viral transduction and GCaMP6s expression

The brains of 3 animals, that were injected with rAAV2/7-CAG-GCaMP6s, were dissected 3 weeks after injection, postfixed in 4% PFA for 10h and dehydrated in 30% sucrose for 3 days at 4°C (Sigma Aldrich, S9378). Brains were sectioned in the coronal plane on a sledge microtome (40 μm). The slides were incubated with primary antibodies anti-GFP (Abcam, ab6556, conc: 1:500) and anti-NeuN (Millipore, Mab377, conc: 1:1000) diluted in 0.3% Triton X-100 (Sigma-Aldrich, T8787) supplemented with 2% donkey serum (Abcam, ab7475) for 10 h at 4°C. After washing with PBS for 3 × 5 min, sections were incubated with secondary antibodies Alexa Fluor 488 anti-rabbit (Thermo Fisher, A-21206) and Alexa Fluor 568 anti-mouse (Thermo Fisher, A10037) for 1h at 4°C (both 1:500 diluted). Sections were counter-stained with DAPI, mounted with fluorescent mounting medium (Dako, S302380) and coverslipped. Slides were imaged using a confocal microscope (Zeiss, LSM 700). The number of GCaMP6s positive cells and NeuN positive cells around the injection site were counted on 3 sections per bird and the transduction rate determined.

Assessing immune response to rAAV2/7-CAG-GCaMP6s injection

The brains of 3 animals were dissected 3 weeks after injection with rAAV2/7-CAG-GCaMP6s, postfixed in 4% PFA, embedded in 4% agarose, sectioned on a vibratome (40 μm) and mounted on coverslips. Antigen retrieval was performed by slow heating of the slides in antigen retrieval buffer (Vector, H-3301) up to 90°C, followed by cooling at room temperature for 40 min. The slides were then incubated with primary antibodies anti-GFP (Abcam, ab6556, conc: 1:500) and anti-GFAP (Invitrogen, Cat#13–0300, conc: 1:500) diluted in 0.3% Triton X-100 (Sigma-Aldrich, T8787) supplemented with 2% donkey serum (Abcam, ab7475) for 10 h at 4°C. After washing with PBS for 3 × 5 min, sections were incubated with secondary antibodies Alexa Fluor 488 anti-rabbit (Thermo Fisher, A-21206) and Alexa Fluor 568 anti-rat (Thermo Fisher, A11077) for 1h at 4°C (both 1:500 diluted). Sections were counter-stained with DAPI, mounted with fluorescent mounting medium (Dako, S302380) and coverslipped. Slides were imaged using a confocal microscope (Leica, Stellaris 5). Maximum intensity projections of acquired z-stacks were generated and mean fluorescent intensities of the GFAP staining measured using Fiji. The mean fluorescent intensity of sections (n = 3) from the ipsilateral and contralateral side of rAAV2/7 injections (n = 3 birds) were compared using a paired, two-tailed t-test. DAPI positive nuclei were counted on the same sections (n = 3) and the mean number of cells in the ipsilateral and contralateral hemispheres (n = 3 birds) compared using a paired, two-tailed t-test.

2-Photon microscopy

In vivo 2-photon calcium imaging was performed on awake animals that were habituated to the experimental set-up for 3 days in advance. We used a custom resonant scanning 2-photon microscope (Neurolabware, Los Angeles, CA) controlled by Scanbox acquisition software (Neurolabware, Los Angeles, CA), a Coherent laser run at 920 nm (Coherent Chameleon, #GDP.1185894.8031) and a 16x water immersion objective with 3 mm working distance (Nikon, #CFI75LWD16XW). 512 lines per frame were acquired at 15.63 Hz in resonant scanning mode. Laser power below the objective was 60–120 mW. Dwell time of the laser was 48 ns per pixel. Table S1 highlights possible issues that might arise while imaging, the cause, and appropriate remedial action.

Light stimulation

Light emitting diodes (JKL Components, #ZFS-105000-24RGB and #ZFS-105000-DBW; Renkforce UV, #1518598) were attached to the wall of the experimental chamber facing the pigeon's front in vertical stripes covering an area of 60 × 40 cm (length/height) with 4 cm spacing. Light of different wavelengths (violet/UV, blue, green, red, white light), diffused through a frosted glass wall, was repeatedly presented to the pigeons for 10 s at total intensities between 9.2 $\mu W/cm^2$ and 10.5 $\mu W/cm^2$ (measured with Spectroradiometer SpectriLight ILT950 at the head position of the animals) followed by 20 s inter-stimulus periods in darkness. Transistor-transistor logic (TTL) pulses were generated by an Arduino for every stimulus on- and off-set and time stamped with the frame number that was acquired at that time.

QUANTIFICATION AND STATISTICAL ANALYSIS

Calcium images were motion stabilized by rigid alignment using the Scanbox align tool (Neurolabware, Los Angeles, CA). Regions of interest (ROIs) were manually selected, and average fluorescence intensities for each frame extracted using Fiji.[58] Background corrected fluorescence values for each frame were computed by subtracting the intensity values of ROIs placed in the background. The change in fluorescence (ΔF/F) was then calculated using the following equation where F_0 is defined as the average fluorescence intensity of the bottom 10% of frames of each ROI:

$$\frac{\Delta F}{F} = \frac{F - F_0}{F_0}$$

Fluorescent traces were linearly interpolated from 15.63 fps to 50 fps (MATLAB *interp1* function) and fluorescence peaks for pre-, and during stimulus periods detected using the MATLAB function *peakdet*. Interpolating the frame rate to full integers (50fps) facilitated binning for statistical analysis. To test for visual responsiveness, the fluorescent peak frequency of individual neurons in the 10 s before and during the 5 different visual stimuli (violet/UV, blue, green, red, white light) were compared using the Kruskal-Wallis test for non-parametric data with Dunn's post-hoc test.